Photochemistry and Photobiology, 2011, 87: 1042–1049

Enhanced Melanin Fluorescence by Stepwise Three-photon Excitation

Josef Kerimo[1], Milind Rajadhyaksha[2] and Charles A. DiMarzio*[1,3]

[1]Department of Electrical and Computer Engineering, Northeastern University, Boston, MA
[2]Dermatology Service, Memorial Sloan-Kettering Cancer Center, New York, NY
[3]Department of Mechanical and Industrial Engineering, Northeastern University, Boston, MA

Received 19 January 2011, accepted 25 May 2011, DOI: 10.1111/j.1751-1097.2011.00949.x

ABSTRACT

The fluorescence of eumelanin (from *Sepia officinalis* and black human hair) was activated and enhanced by almost three orders of magnitude by exposure to near-infrared radiation. No activation or enhanced emission was observed when the samples were heated up to 100°C. The near-infrared irradiation caused obvious changes to the eumelanin and could be seen by fluorescence and bright field imaging. The area of enhanced emission appeared to originate from a region with changes in the morphology of the eumelanin's granule and increased with exposure time. At least two different components with enhanced fluorescence were activated and could be distinguished by their excitation properties. One component could be excited efficiently with wavelengths in the visible region and exhibited linear absorption dependence with respect to the laser power level. The second component could be excited efficiently using near-infrared wavelengths by a nonlinear process and exhibited a third-order dependence on the excitation. The third-order dependence is explained by a step-wise excited-state absorption process since the same third-order dependence was present when either continuous wave or femtosecond pulsed laser, with similar average-power levels, was used.

INTRODUCTION

Naturally occurring pigmentation that determines hair, eye and skin coloration is attributed to two types of melanin: eumelanin and pheomelanin. Eumelanin is the dominant component of brown and black pigments in dark skin and black hair while pheomelanin is more common in yellow and red pigments in hair (1). Both pigments serve an important role as natural sunscreens and protect against UV radiation by an efficient process that converts the absorbed light to heat. However, the exact role of melanin's activity is not known, as it has also been known to produce free radicals in response to the UV radiation, which may be toxic (2). In addition, the pigments appear to exhibit many properties such as photoconductivity that appear to have no known biological significance. However, it is clear the optical properties of melanin play an important role in its function.

The molecular structure and organization of melanin are complicated and not completely known. In humans, the melanin is synthesized within membrane-bound vesicles called melanosomes by melanocytes and appears to be about a few hundred nanometers to several micrometers in size (3). Atomic force and scanning electron microscopy have shown that the organization of melanin into various sizes, from tens of nanometer to micro meters, plays an important role in its function and photophysics (4). For example, it has been shown that the amount of melanin aggregation determines its ability to generate active oxygen species (5,6). One of the goals of this work is to develop optical microscopic techniques that can be used to study the optical properties of individual melanin structures.

Our approach is to use fluorescence to detect the melanin and probe its photophysics. In general, melanin is considered a weak emitter with a very low quantum yield of fluorescence, less than 10^{-3} (7). Since the fluorescence from melanin is difficult to detect, it has been largely ignored in fluorescence microscopy. The poor emission is explained by the rapid decay of the excited-state population through nonradiative processes to the ground state, which typically occurs within a few picoseconds (8). The emission spectrum is also reported to change with the excitation wavelength, which is unusual for fluorophores. Its absorption spectrum is broad, feature-less and decays exponentially from the UV to the near-infrared. Both the emission decay and ground state recovery have a nonexponential trend and may indicate the presence of several different species (6,8). The complicated photophysics of melanin could be due to the heterogeneity of the melanin sample. This can be alleviated by using optical imaging methods to probe individual melanin structures.

Various microscopy methods have been used to study melanin *in vivo* and *in vitro*, but there has been little work with fluorescence because it is difficult to detect. However, under certain conditions, the fluorescence from melanin can be enhanced by several orders of magnitude by using strong oxidizing agents and UV excitation (9,10). Since UV excitation is required before the enhanced emission is observed, it is possible that pulsed near-infrared light, through a multiphoton excitation process, can generate the same enhanced fluorescence. The advantage of this approach is that the enhanced melanin emission can be triggered *in vivo,* which is more practical for imaging of biological samples. Here, we report our preliminary results in generating enhanced melanin emission with near-infrared light. For most of our samples, the emission from melanin was initially almost undetectable on our microscope with either visible or near-infrared laser excitation. Strong emission from melanin could be observed

*Corresponding author email: dimarzio@ece.neu.edu (Charles A. DiMarzio)

only after it was first illuminated with a high level of near-infrared light (pulsed or continuous wave [CW]), which lead to changes in the melanin structure and enhanced emission that saturated the detectors.

We also studied the dependence of the enhanced emission on the illumination power. In prior studies, the oxidized and UV-treated melanin was reported to have a linear dependence with visible light excitation (9) while the untreated melanin had second-order dependence with pulsed near-infrared light excitation (11). The second-order dependence was attributed to a step-wise excited-state absorption (ESA) which is different from conventional multiphoton absorption. It is not clear whether the melanin exhibiting ESA is the same as the one with linear dependence or whether there are multiple emissive components. For this reason, the melanin was imaged on the microscope to determine the presence of different species and their power dependence at different excitation and emission wavelengths. We present the first fluorescence images of the enhanced emission, caused by near-infrared radiation, from *Sepia officinalis* and black human hair melanin.

MATERIALS AND METHODS

Samples. The eumelanin sample form Sepia was purchased from the Sigma Chemical Company and was used without further processing. This sample contained the pure form of eumelanin, which is extracted from the ink sacs of the squid *Sepia officinalis* and has almost no other residues or components that could interfere by fluorescence. It served as the reference standard for our melanin sample. The sample comes in the form of a black powder and is insoluble in most solvents but could be spread on a microscope coverslip in a dry form. Individual granules of melanin could be observed and ranged in size from less than a micrometer to tens of micrometers and were mostly spherical or oval in shape. It was not possible to see any fine structures on the granules since their surface was mostly smooth and showed no indication of aggregation. Naturally occurring melanin structures in melanosomes are typically smaller and are *ca* a hundred nanometers in size.

The other sample studied in this work was natural fibers of black human hair, *ca* 50 μm in diameter, and were used without any treatment or modification. The black human hair was imaged on the microscope to see if it was possible to detect the emission from melanin in its natural state.

The samples were sometimes mounted inside culture dishes so that the air could be purged out with nitrogen, to reduce photobleaching. This was especially important for the power dependence measurements. When the sample was placed in nitrogen the emission was very stable and the duration of the emission increased from a few milliseconds to almost a minute. The dishes were also used to control the temperature and were used to determine the effect of high temperatures on the melanin emission. The closed chamber system and the dishes were from Bioptechs (Butler, PA).

Microscopy. A home-built laser scanning confocal microscope was used to image the samples. A detailed description of the microscope system can be found elsewhere (12). The system is based on an inverted Nikon microscope and a fast polygonal-galvanometric scanning system. The polygon scanner performs fast scanning along a linear direction with line speeds of *ca* 6 kHz and pixel dwell time of 200 ns while the galvanometer scans the line in the perpendicular direction, resulting in an imaging rate of 10 frames per second. The galvanometer can also be turned off so that the polygon scanner performs continuous line-scanning at a select location on the sample. In this configuration, a fixed line is scanned continuously across the sample and the signal from the line is averaged and plotted *versus* time. The line-scanning method was required for some of the experiments in order to study rapid changes in the fluorescence signal that could otherwise not be captured with the slower frame-scanning mode. All of the imaging was done with three types of Nikon Plan Apo microscope objectives: 20 × 0.75 NA and 60× or 100 × 1.45 NA.

Laser excitation sources. A near-infrared pulsed laser was used to induce the enhanced emission from the melanin and to perform the multiphoton fluorescence imaging in either pulsed or CW mode. The enhanced emission could be generated equally well in pulsed or CW mode using the same average laser power level. The near-infrared laser consisted of a mode-locked Ti:sapphire pumped laser system (Tsunami) from Spectra Physics operating at 80 MHz pulse repetition rate. The pulses were 100 fs in width and could be tuned from 700 to 980 nm. The mode-locking system of the Ti:sapphire laser was sometimes disabled to switch it to CW mode of operation, which was required for some of the experiments. The CW operating mode was confirmed by the narrow spectral bandwidth of the laser output as well as the lack of two-photon fluorescence on standard samples.

A CW visible laser was also used in the confocal fluorescence imaging and could be tuned to a single laser line between 454 and 514 nm. Because of the unique multimodal configuration of the microscope, the same area on the sample could be imaged with either the near-infrared or visible laser with the images being fully registered.

Detection system. Photomultipliers (PMT's: Hamamatsu, HC124-02) were used to detect the emission in the visible region. Bandpass filters in front of the PMT's selected the emission band (see Table 1) and the output of the PMT amplifier was digitized directly by a frame grabber card in the computer (National Instruments PCI-1408). The emission in the near-infrared region was detected with a CCD camera (SPOT RT900). High quality edge filters, centered at 785 nm, were used to block the laser and to pass the near-infrared emission to the camera (Semrock, LPD01-785RS and LP02-785RS). The linearity of the detection system was tested and corrected, as needed, by software.

Power dependence measurements. Power dependence measurements were obtained by modulating the laser excitation power while detecting the fluorescence. The fluorescence and laser level were recorded simultaneously and used to produce the power dependence plots. In these experiments, the sample was first imaged with the polygonal-galvanometric laser scanning system to determine the area of interest. The galvanometer was then turned off and parked at the desired location on the sample for line-scanning and laser power modulation. The laser power was measured with a calibrated silicon photodiode (Newport, 1830-C) and all laser power levels refer to power measurements taken at the sample.

Imaging and power dependence experiments. All the experiments were performed on the microscope where the samples were first exposed to the near-infrared radiation, to activate the emission and then imaged. The activation was done with the laser in pulsed or CW mode and the wavelength ranged from 700 to 980 nm. The power dependence was recorded on regions that showed enhanced emission. In order to distinguish different components with activated emission, we used different parameters for the imaging and power dependence experiments such as excitation and detection at different wavelengths, and pulsed or CW laser excitation; for convenience, all the parameters are listed in Table 1. Note that Table 1 divides the imaging (imaging 1 and imaging 2) and power dependence (power dependence 1 and power dependence 2) experiments according to the two different laser excitation sources used here.

In an effort to study morphological changes to the melanin particles due to the near-infrared radiation, the samples were also imaged in the brightfield and epifluorescence modes with high magnification. Sepia melanin particles were placed in nitrogen atmosphere and then briefly exposed to 930 nm laser irradiation to activate the emission. The same

Table 1. Experimental parameters for imaging the enhanced emission of melanin and determining the laser power dependence. The measurements were done on the Sepia and hair samples.

Experiment	Laser (nm)	Laser modes	Emission (nm)
Emission activation	700–980	Pulsed, CW	
Imaging 1	454	CW	480–650
Imaging 2	700–980	Pulsed, CW	400–650, > 785
Power dependence 1	454	CW	480–650
Power dependence 2	700–980	CW, pulsed	400–650, > 785

CW = continuous wave.

area was then imaged with the 100× objective and the two registered images were overlaid to visualize changes to the melanin morphology and the source of the activated fluorescence.

RESULTS

Laser power dependence of the enhanced emission

Two different emissive components could be observed based on the excitation wavelength and the power dependence of the emission from Sepia melanin. The power dependence of the two components is shown in Fig. 1; the data from different samples, modes of excitation, and emission and excitation wavelengths are presented. (The fluorescence images corresponding to the two different components were also collected but are shown later in Fig. 2). One of the components could be excited efficiently with visible light (454 nm) and had linear power dependence (Fig. 1a); while the other component could be excited efficiently with near-infrared light and femtosecond pulses and had third-order power dependence (Fig. 1b). Previous work reported a linear (10) and second-order power dependence (11) for visible and near-infrared excitation, respectively, but there has been no report of a third-order power dependent component in the melanin emission. Our data could be fit with just a third-order function alone. There was no evidence of the second-order component. The third-order power dependence shows that the emission is generated by an excitation process that requires three photons.

The component with linear power dependence (Fig. 1a) could not be excited by multiphoton absorption using near-infrared light. It could only be excited with the 454 nm laser. For example, when the laser was switched to femtosecond mode and tuned to 900 nm, roughly twice the wavelength of the 454 nm laser, there was no emission from this component. This indicates that it had a low two-photon absorption cross-section or inefficient step-wise two-photon absorption. It

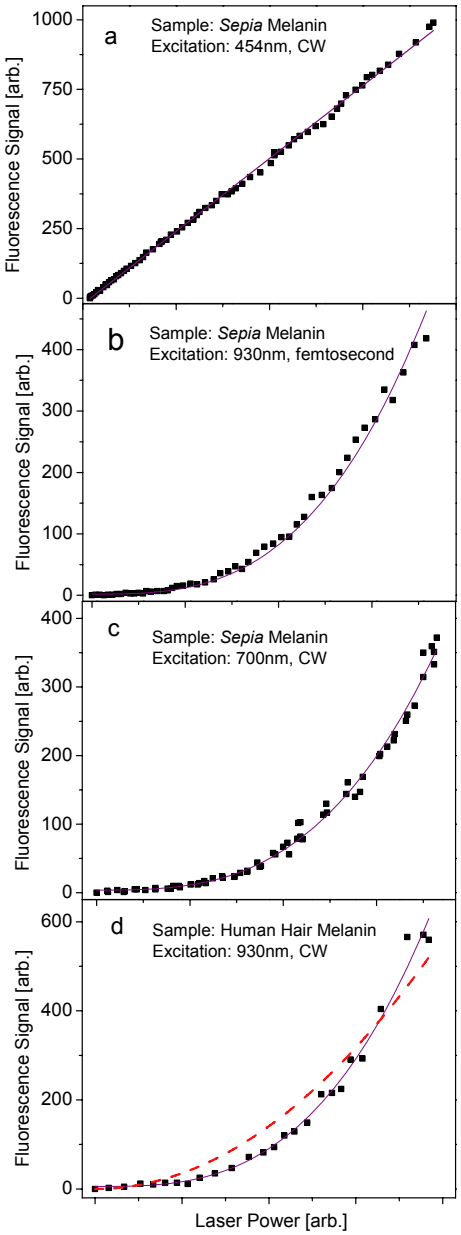

Figure 1. Plots of the fluorescence signal *versus* laser power. Solid lines represent third-order polynomial fit except for (a) which is a straight line fit. The dashed line in (d) is a second-order fit. The labels show the corresponding pulsed or continuous wave (CW) laser excitation and sample. The 480–650 nm emission was detected for all.

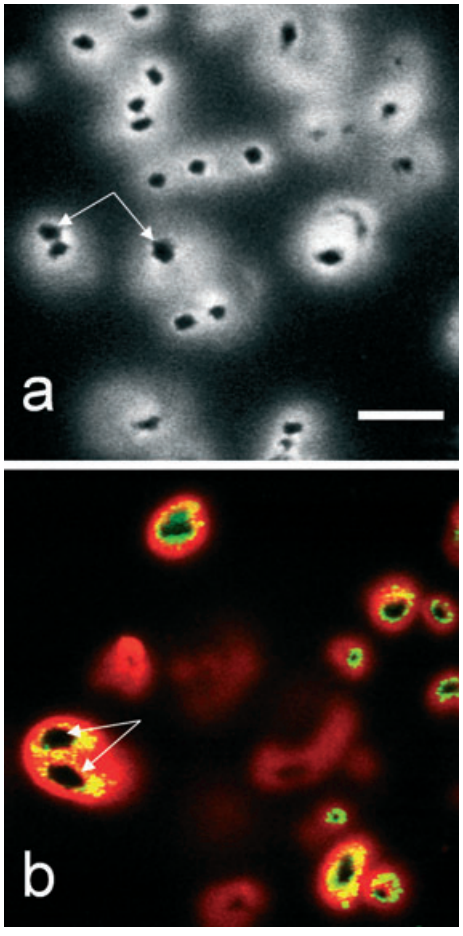

Figure 2. Fluorescence from Sepia melanin. (a) Visible emission (480–650 nm) with 454 nm laser excitation. (b) Pseudocolor image of emission from 454 nm (red color) and 760 nm laser excitation (green color). The scale bar is 10 μm.

appears the linear component is completely different from the second-order component reported in the literature and the third-order component seen here.

For the other emissive component (third-order power dependence with the femtosecond near-infrared laser) the fluorescence could also be observed when the near-infrared laser was switched to CW mode (Fig. 1c). The laser power dependence remained third order. This behavior was seen across the whole tuning range of our laser (700–980 nm). Interestingly, the emission signal was reduced by only a small amount when the laser was switched from femtosecond to CW mode. For example, equivalent fluorescence signal level was observed for average-power level of 0.2 mW (1×10^4 W cm^{-2}) in pulsed mode and 0.46 mW (3×10^4 W cm^{-2}) in CW mode at 930 nm. The equivalent peak power level of the laser excitation for this example was 12500 mW (7×10^8 W cm^{-2}) for pulsed excitation. This indicates that the peak power played only a minor role and femtosecond pulses were not required to see the emission from this component. Furthermore, the large range of the third-order dependent excitation (700–980 nm) shows a broad range of excited states and the highest were between 233 and 326 nm.

We used 770 nm CW excitation to determine the power dependence of the near-infrared emission (>800 nm). The power dependence of the near-infrared emission was third order and not linear (data not shown).

Two different emissive components were also seen on the black human hair sample and they had similar power dependence as the pure Sepia melanin. Figure 1d shows the power dependence of one of the components of this sample. The data was taken with the laser set to 930 nm and in CW mode and was fit to a third-order function. For comparison, a second-order fit is also included in Fig. 1d to show that it does not represent the power dependence data. The other emissive component for the hair sample had similar linear power dependence as the Sepia melanin and could be excited with the 454 nm laser.

Imaging Enhanced Emission from Sepia Melanin

Before the Sepia melanin was exposed to the near-infrared light, there was little or no detectable emission on the microscope. When the sample was excited with the 454 nm laser and up to 43 μW (1×10^4 W cm^{-2}) of illumination power, we did not detect any fluorescence. Similarly, no fluorescence could be detected when femtosecond near-infrared radiation, up to 0.2 mW (peak power density 7×10^8 W cm^{-2}) at the sample, was used. It is possible the emission was present but was too weak or below the detection threshold of our microscope. The emission from the Sepia melanin could only be observed after the near-infrared laser light was increased above a certain threshold, *ca* 0.2–0.3 mW at the sample, and the emission became visible to the eye, appeared yellowish and saturated the detector.

Following the near-infrared laser exposure, the samples were again imaged with the visible laser at 454 nm but at a much lower excitation intensity level, 0.75 μW instead of 43 μW. At the much lower illumination power, an emission could be seen that was not present earlier. The fluorescence confocal image of this emission, 480–650 nm, is shown in Fig. 2a. Individual melanin particles, measuring several micro meters in size, were clearly seen by the strong fluorescence signal but no structures or aggregation could be resolved except for the large ''dark'' nonfluorescent areas (arrows on Fig. 2a). The activation of the enhanced emission could be done with the near-infrared laser operating in CW or pulsed mode and with almost the same average-power level. This indicates the activation process did not depend on the peak laser power but on the average laser power.

Figure 2b shows a colored image of the enhanced fluorescence taken on two separate imaging experiments on the same area: one was taken with the 454 nm laser (red color) and the other with the near-infrared laser at 760 nm (green color). Note that the fluorescence from the 760 nm laser appears to be more structured and concentrated around the ''dark'' nonfluorescent region (arrows on Fig. 2b). These features were seen on most melanin particles. There was very little emission by the 760 nm laser beyond the immediate region of the dark features. In some cases, it was possible to see emission from the dark regions using the near-infrared laser if the photobleaching was reduced, and the imaging was done at multiple focal planes. When the melanin was imaged in a nitrogen atmosphere, to slow down photobleaching effects, the emission from the dark region could clearly be seen with the near-infrared laser but from a limited focal plane. This is due to the fact that the fluorescence generated by the near-infrared laser was due to a multiphoton process and detected from a smaller focal volume than the confocal setup, or 454 nm excitation. It seems the ''dark'' regions were caused by rapid photobleaching or the emissive material was simply out of focus. Finally, there was also an increase in the near-infrared fluorescence with the near-infrared laser (data is not shown) and the images had similar dark features.

Clearly, we could see two different species that exhibited enhanced emission when the melanin was activated and they could be distinguished by their absorption properties. One of the species was excited by a nonlinear absorption process with near-infrared wavelength while the other linearly with visible wavelength. Furthermore, the morphology of the two components was very different on the images. One of the components had a smooth morphology with few features while the other component appeared granular and mostly around the dark regions.

The sepia melanin was imaged with high magnification in brightfield and epifluorescence mode to determine whether the near-infrared laser caused any changes to the morphology of the particles and whether the whole melanin particle became fluorescent. It was not possible to determine the physical extent of the activated emission across the melanin particle with just the fluorescence image. For this reason, the brightfield image was collected and overlaid on the fluorescence image. A pseudocolor image is shown in Fig. 3a with the epifluorescence in green and the brightfield in red. The emission in this case was excited with visible light, 420 nm, and mapped the linearly excited component. The ''dark'' region and the changes to the melanin particle can be better seen if the brightfield image was overexposed to overcome the strong absorption of melanin (Fig. 3b). It is clear from these images that the emission does not come from the whole melanin particle but only from a limited area. Furthermore, it appears the near-infrared laser caused changes to the melanin particle and the enhanced emission appears to originate from these regions.

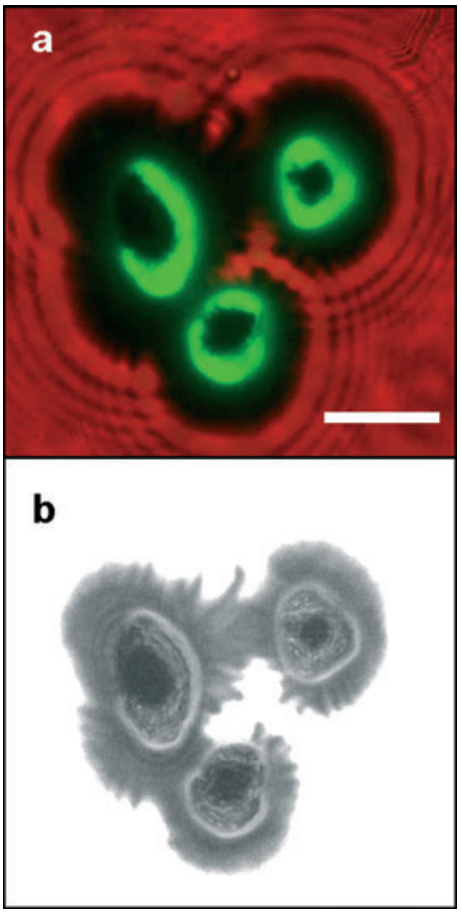

Figure 3. Epi fluorescence and brightfield images of Sepia melanin. The fluorescence was excited at 420 nm and detected at 525 nm: (a) pseudocolor image of the epi fluorescence (green) and the brightfield (red) images and (b) brightfield image of the same sample but with enhanced brightness. Scale bar is 5 μm.

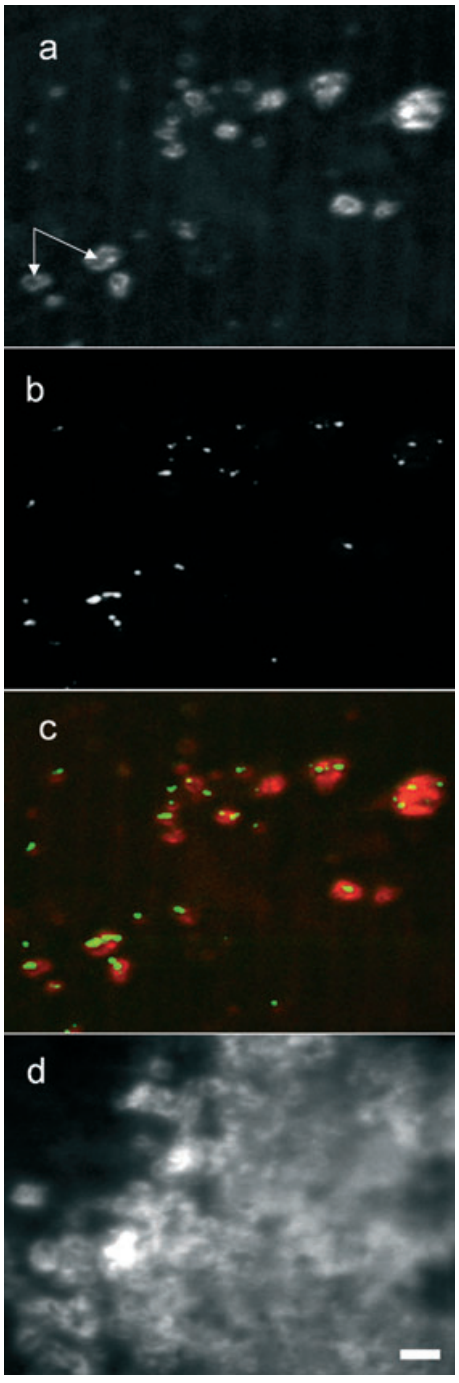

Figure 4. Fluorescence images of human hair melanin. For all images, 480–650 nm emission was detected. The same area was imaged, showing (a) a confocal fluorescence image excited at 454 nm, (b) a fluorescence image excited with a 930 nm pulsed laser, (c) a pseudo-color image of 454 nm exctitation in red and 930 nm excitation in green and (d) same as in (a) but after longer exposure to the 930 nm laser. Arrows indicate ''darker'' regions. Scale bar is 5 μm.

Imaging human hair melanin

Just like the Sepia melanin, it was possible to observe emission from the hair sample only after the near-infrared laser light activated the emission above a certain threshold. For example, there was no emission from the hair when it was excited with just the 454 nm laser or the near-infrared laser at the lower power setting (up to 0.5 mW and femtosecond pulses at 930 nm). When the near-infrared laser intensity was increased above 1 mW (3.5×10^9 W cm^{-2}) it was possible to see the emission (Fig. 4). Note that a somewhat larger laser power was required to activate and image the enhanced fluorescence in hair relative to the Sepia sample. In hair, the melanin is located inside the hair matrix and some of the laser power is lost due to scattering before the excitation. For comparison, the hair sample required a factor of eight higher laser power at 454 nm and a factor of 2 at the near-infrared wavelength to reach the same fluorescence signal level as the Sepia melanin. The factor of 2 for the near-infrared radiation is consistent with a multiphoton excitation that has third-order dependence in the near-infrared region.

Figure 4a is the fluorescence image of the linearly excited hair melanin using the visible laser and Fig. 4b is the corresponding image using three photons with the near-infrared laser. Just like the Sepia melanin, the emissive features are similar in shape and contained ''darker'' regions with less emission (arrows on Fig. 4a). The darker regions are attributed to emissive species that can only be excited with

the near-infrared laser and not the visible laser; this can be seen from the combined image presented in pseudocolors (green and red) in Fig. 4c with perfect registration of the dark regions and the three-photon emission (green color). Furthermore, the emission excited by the near-infrared laser seemed to originate from highly localized regions that were diffraction limited in size while the emission excited by the visible laser was more uniform and spread out just like the Sepia melanin. The number of melanin granules that were activated also increased with exposure to the near-infrared laser. Figure 4a is the image after 2 s of illumination and Fig. 4d is the same area but after 20 s illumination. For Fig. 4d, the focus was also varied to activate the emission from several different layers.

DISCUSSION

There have been many studies done on the autofluorescence of melanin, both *in vitro* and *in vivo* (11,13), but rarely in the microscopy imaging modes employed here. The emission from melanin is normally weak and not easy to observe since the absorbed light is converted to either heat or excited-state photochemistry. Furthermore, the melanin emission photobleached quickly in air and was not easy to study. In this work, we have shown that melanin could be turned into an efficient emitter after it was first irradiated with intense near-infrared light and the photobleaching was reduced considerably in a nitrogen atmosphere. Furthermore, we could not detect any melanin emission before this irradiation. We estimate the emission improved by at least three orders of magnitude. This level of improvement is consistent with the enhanced emission reported elsewhere (9), where both UV exposure and chemical oxidation of melanin was required. In contrast, our enhanced emission could be observed in a nitrogen atmosphere which lacked the main oxidation component or oxygen. It appears the higher energy excited state is more important for generating the enhanced emission than the chemical oxidation step.

Heat could play an important role in generating the new emissive species in the activated melanin. Melanin is a strong light absorber and is known to convert the excited light into heat. It is possible the near-infrared laser simply heated the melanin to high temperatures, which lead to changes in the morphology and enhanced emission. For this reason, both the Sepia melanin and hair samples were heated up to 100°C to determine if there were any improvements in the emission. For the Sepia melanin sample we did not see any enhancement in the emission after the heat treatment. A small improvement in the emission of the hair sample was observed but it had different properties. The new emission from the heat treated hair could only be seen when the laser was in pulsed mode and not in CW mode, and it was distributed uniformly. Although the samples were heated up to 100°C (limited by our instrumentation) and we observed no enhanced emission, it is not possible to rule out activation at higher temperatures. Future work is planned to determine the upper range of the temperature (modeling the heat) and its effect in melanin when using near-infrared light.

The enhanced emission was more likely initiated by absorption of several near-infrared photons. Evidence of the initial multiphoton absorption step was seen by the localization of the enhanced emission in the focal direction of the microscope images. If the activation was not initiated by a multiphoton process but by a linear absorption step then emission would have been activated along the z-direction and beyond the resolution of the microscope. For a multiphoton process, it should be localized to a thin resolution element. The fluorescence signal on our images was always localized within thin z-sections in the focus direction that measured *ca* 1 μm in thickness. This is comparable to the z-resolution of our three-photon fluorescent image which was estimated to be *ca* 0.8 μm; this strongly points to a multiphoton activation step. Furthermore, the activation step was previously reported to require UV exposure (9) but here it was observed with near-infrared light up to 980 nm. Assuming the same excited state was reached for both cases then the near-infrared activation was through a three-photon absorption (TPA) process.

One of the emissive species in melanin had a third-order fit for its laser power dependence, indicating it was excited predominately by three photons with a final excited state in the UV region. Further evidence of the third-order dependence could also be seen from the range of the emission wavelength for this component. When the laser was tuned to 980 nm we could observe emission between 435 and 485 nm which is well above the two-photon excitation energy. This indicates the activated emission from this specie must be produced by a process higher than second order. This is the first reported evidence of three-photon fluorescence from melanin.

Recently, near-infrared fluorescence from melanin was reported with 785-nm laser excitation and the emission was used as a novel tool for *in vivo* tissue evaluation (14,15). It was thought that the near-infrared emission was caused by a linear excitation process but the power dependence was not measured. In this work, we confirm that there was near-infrared emission in the activated emission and its power dependence was third order. We expect the near-infrared emission to originate from the same set of excited states as the emission in the visible region since they had the same power dependence. It is surprising that we did not see a linear dependence in the near-infrared emission considering that we used a CW laser at 770 nm and detected the >800 nm emission. For this example, the near-infrared emissive component was excited by three photons (equivalent to 260 nm excitation) and the emission was broad and could be detected from 435 nm and all the way to 800 nm or more. More work is needed to determine if the near-infrared emission represents a different component or simply reflects the decay of the excited state.

The third-order power dependence is unlikely due to traditional TPA since this process is very inefficient and requires pulsed lasers. In TPA, the excitation goes through one or more virtual states to reach the final excited state. Femtosecond lasers with very high peak intensity are used in order to make the multiple virtual-state transitions. A diagram of the TPA process and the corresponding virtual states is shown in Fig. 5 inset. In this work, TPA could be seen with both the femtosecond and CW laser using the same average laser power. It appears the peak laser power levels played only a minor role in determining the emission and the excited-state population and conclude that traditional TPA was not important here.

One explanation for the lack of dependence on the laser peak power is that the melanin makes the excited-state transitions through real states and not virtual states or by ESA. Figure 5 inset shows how individual absorption steps

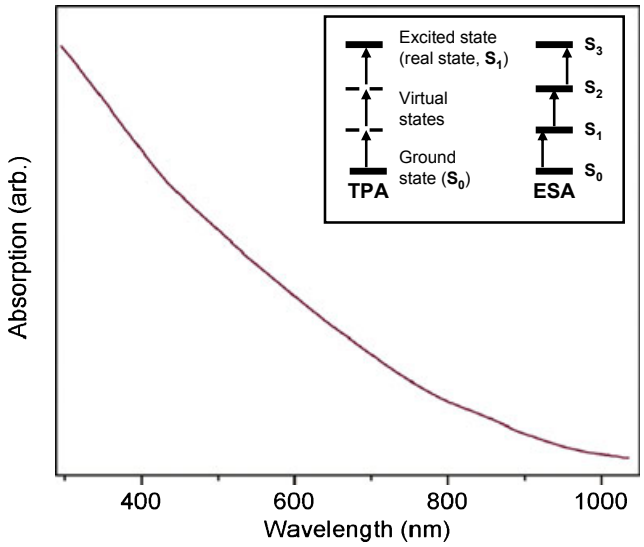

Figure 5. Absorption spectrum of Sepia melanin (adapted from Ref. 21). Inset shows two different types of three-photon absorption processes (TPA = three-photon absorption; ESA = excited-state absorption) where solid horizontal lines are real states and dashed lines are virtual states.

with linear dependence (three in this case) lead to the ESA process. The idea of an ESA process for melanin is not new since second-order dependence has been reported but the evidence was not conclusive (11). The prerequisite for ESA is the existence of intermediate real states, such as S_1 and S_2 in Fig. 5, which can absorb light in the excited state. Melanin has a broad absorption curve that extends from the UV into the near-infrared region and can support such states, as seen in the absorption curve in Fig. 5. In this work, it was possible to activate and excite the melanin emission anywhere from 700 to 980 nm by a third-order power dependent process using almost the same average-power threshold for the pulsed and CW laser. The wide range of activation and excitation is due to the broad absorption curve of melanin. The lack of dependence on pulsed or CW radiation indicates that the ESA process is the underlying mechanism.

The relationship governing the three-photon ESA signal was derived elsewhere (16) and is given by

$$N_3^{ss} = \tau_1\tau_2\tau_3\left(\frac{\lambda}{hc}\right)^3\sigma_0\sigma_1\sigma_2 N_0 P_{ave}^3$$

N_3^{ss} is the steady-state population of the highest excited state, σ_i and τ_i are the absorption cross-section and lifetime of state i, respectively (see Fig. 5 for labeling of the various states). As can be seen from this relationship, the ESA signal does not depend on the peak laser power but on the average laser power P_{ave} and explains our observations. Furthermore, the third-order dependence on P_{ave} makes it possible to conduct nonlinear fluorescence imaging of melanin with just a CW laser.

The first report of ESA-based fluorescence from melanin mentioned only two-photon absorption with a second-order power dependence using femtosecond laser pulses. Interestingly, the same work also stated that the emission could only be seen with femtosecond pulses and not with the longer picosecond or nanosecond pulses (11). If the melanin emission was due to an ESA process then emission should still be observed when the laser was switched to nanoseconds or even CW excitation, as shown here. For this reason it is unclear whether the original report is explained by an ESA process.

Long-lived excited-state lifetimes can improve the ESA efficiency but are not required. Most systems that exhibit efficient ESA, such as common upconversion compounds, have a relatively long lifetime in the range of milliseconds or microseconds (17). Although long-lived melanin species that last several hundred nanoseconds have been observed it is not possible to say if the same long-lived species are present in the melanin with the enhanced emission (5,18,19). We have not measured the excited state lifetime of the melanin but expect it to be longer than the fluorescence lifetime of traditional fluorophores which consists of a few nanoseconds. Based on the appearance of melanin on the fluorescence microscope images (no streaks) and the pixel dwell time we expect the emission lifetime to be shorter than 400 ns and not in the microseconds or milliseconds range that is more common in upconversion compounds. More work is planned to characterize the fluorescence spectra and lifetime of the enhanced emission to determine the nature of the emissive excited state and any additional components in the sample.

The enhanced melanin emission could potentially be used in clinical applications to study most forms of melanin and to map their location. Melanin is an important component in skin and hair, tissues of the eye and ear and the central nervous system and provides protection from radiation and toxic agents. Skin disorders such as vitiligo, melanocytic nevus and melanoma are associated with melanin production and can easily be screened by detecting their enhanced emission. Although melanin is present in various forms and structures, it is very likely the emission for all forms can be enhanced using near-infrared radiation. In this work we have studied eumelanin exclusively and have not studied the other forms of melanin. However, it has been found that enhanced emission by oxidation and UV radiation could be induced for other types of pigments such as pheomelanin, neuromelanin, ochronotic pigment and synthetic melanin (20). In all these cases, the enhanced emission had the same properties and it is very likely they share the same mechanism and fluorophore.

Based on the similarities of the power dependence of Sepia melanin and black human hair, it is reasonable to conclude that the enhanced emission from the black human hair was also due to melanin and not other components. Since the emissive features in the hair sample looked very similar to the Sepia sample, which contains pure melanin, we believe it was due to the melanin granules and not other emissive components. Further support of this comes from the melanin coverage in the hair, as presented in the microscope images in Fig. 4. Black human hair is reported to contain *ca* 1–3% melanin (1) which is close to the 2% estimated from the fluorescence image in Fig. 4a.

REFERENCES

1. Robbins, C. R. (2002) *Chemical and Physical Behavior of Human Hair*. Springer, New York.
2. Felix, C. C., J. S. Hyde, T. Sarna and R. C. Sealy (1978) Melanin photoreactions in aerated media: Electron spin resonance evidence for production of superoxide and hydrogen peroxide. *Biochem. Biophys. Res. Commun.* **84**, 335–341.

3. Tolleson, W. H. (2005) Human melanocyte biology, toxicology, and pathology. *J. Environ. Sci. Health Part C Environ. Carcinog. Ecotoxicol. Rev.* **23**, 105–161.
4. Liu, Y. and J. D. Simon (2003) Isolation and biophysical studies of natural eumelanins: Applications of imaging technologies and ultrafast spectroscopy. *Pigment Cell Res.* **16**, 606–618.
5. Nofsinger, J. B., S. E. Forest and J. D. Simon (1999) Explanation for the disparity among absorption and action spectra of eumelanin. *J. Phys. Chem. B* **103**, 11428–11432.
6. Nofsinger, J. B. and J. D. Simon (2001) Radiative relaxation of Sepia eumelanin is affected by aggregation. *Photochem. Photobiol.* **74**, 31–37.
7. Meredith, P. and J. Riesz (2004) Radiative relaxation quantum yields for synthetic eumelanin. *Photochem. Photobiol.* **79**, 211–216.
8. Nofsinger, J. B., T. Ye and J. D. Simon (2001) Ultrafast nonradiative relaxation dynamics of eumelanin. *J. Phys. Chem. B* **105**, 2864–2866.
9. Kozikowski, S. D., L. J. Wolfram and R. R. Alfano (1984) Fluorescence spectroscopy of eumelanins. *IEEE J. Quantum Electron.* **20**, 1379–1382.
10. Kayatz, P., G. Thumann, T. T. Luther, J. F. Jordan, K. U. Bartz-Schmidt, P. J. Esser and U. Schraermeyer (2001) Oxidation causes melanin fluorescence. *Invest. Ophthalmol. Vis. Sci.* **42**, 241–246.
11. Teuchner, K., J. Ehlert, W. Freyer, D. Leupold, P. Altmeyer, M. Stucker and K. Hoffmann (2000) Fluorescence studies of melanin by stepwise two-photon femtosecond laser excitation. *J. Fluoresc.* **10**, 275–281.
12. Warger, W. C., G. S. Laevsky, D. J. Townsend, M. Rajadhyaksha and C. A. DiMarzio (2007) Multimodal optical microscope for detecting viability of mouse embryos in vitro. *J. Biomed. Opt.* **12**, 044006.
13. Eichhorn, R., G. Wessler, M. Scholz, D. Leupold, G. Stankovic, S. Buder, M. Stucker and K. Hoffmann (2009) Early diagnosis of melanotic melanoma based on laser-induced melanin fluorescence. *J. Biomed. Opt.* **14**, 034033.
14. Han, X., H. Lui, D. I. McLean and H. S. Zeng (2009) Near-infrared autofluorescence imaging of cutaneous melanins and human skin in vivo. *J. Biomed. Opt.* **14**, 024017.
15. Huang, Z. W., H. S. Zeng, I. Hamzavi, A. Alajlan, E. Tan, D. I. McLean and H. Lui (2006) Cutaneous melanin exhibiting fluorescence emission under near-infrared light excitation. *J. Biomed. Opt.* **11**, 034010.
16. Pollnau, M., D. R. Gamelin, S. R. Luthi, H. U. Gudel and M. P. Hehlen (2000) Power dependence of upconversion luminescence in lanthanide and transition-metal-ion systems. *Phys. Rev. B* **61**, 3337–3346.
17. Auzel, F. (2004) Upconversion and anti-stokes processes with f and d ions in solids. *Chem. Rev.* **104**, 139–173.
18. Forest, S. E. and J. D. Simon (1998) Wavelength-dependent photoacoustic calorimetry study of melanin. *Photochem. Photobiol.* **68**, 296–298.
19. Fu, D., T. Ye, T. E. Matthews, G. Yurtsever and W. S. Warren (2007) Two-color, two-photon, and excited-state absorption microscopy. *J. Biomed. Opt.* **12**, 054004.
20. Elleder, M. and J. Borovansky (2001) Autofluorescence of melanins induced by ultraviolet radiation and near ultraviolet light. A histochemical and biochemical study. *Histochem. J.* **33**, 273–281.
21. Wolbarsht, M. L., A. W. Walsh and G. George (1981) Melanin: A unique biological absorber. *Appl. Opt.* **20**, 2184–2186.